EVLA Memo 115

Tools for Ionospheric Studies

W. D. Cotton

NRAO [1]

Abstract

The ionosphere is a major source of phase errors at low radio frequencies. The ionosphere is not well understood on size scales of a few to a few hundred km at levels that cause major errors for radio astronomical observations. It also follows that astronomical observations of bright sources can be used to study the ionosphere on the size scale of the array and with a sensitivity exceeding that which can be obtained using the GPS satellites. This report describes techniques for extracting information about the structure of the ionosphere from astronomical observations. Examples are given using the Obit package.

Contents

List of Figures

1.1 Introduction

At frequencies below a few hundred MHz the ionosphere becomes a major source of corruption of cosmic signals; determining and removing the effects of the ionosphere is one of the major challenges for high sensitivity, high resolution instruments working at low frequencies such as the VLA and the future LOFAR and LWA arrays. The ionosphere is largely ionized by ultraviolet radiation from the sun which gives it a large diurnal variation. The ionosphere also responds to interactions with the solar wind which can give a variety of moving structures on a range of physical and temporal scales.

At low frequencies, radio telescopes illuminate large regions of the ionosphere; the phase errors induced by the ionosphere can vary both across the field of view and across the array. A calibration technique applicable when the ionospheric phase varies across the field of view but only has linear gradients across the array is described by [3], [2] and [1]. For more complex cases arising from a more disturbed ionosphere, e.g. longer baselines or lower frequencies, new techniques need to be developed. In order for this to happen, the properties of the ionosphere on the relevant scales need to be better understood. Since astronomical signals are strongly affected by the ionosphere, these signals can be used to study the ionosphere. This report explores several techniques. Examples are given using the Obit package (http://www.cv.nrao.edu/~bcotton/Obit.html) with AIPS to display the results.

1.2 Observations of Bright Radio Sources

Observations by radio interferometers give visibilities that are integrals over the field of view of the array elements and in general include contributions from a number of sources with a range of strengths. Since the ionospheric phase corruption is spatially and temporally variable, the phase relation between the various sources is unpredictable and variable.

The situation is greatly simplified if the field of view is dominated by a single bright source. In this case, the interferometric measurements can be used to derive the relative, total electron content (TEC) along the lines of sight from the various elements to the source. Thus, at any instant, a set of puncture lines through the ionosphere with the size and geometry of the observing array may be obtained. Since an interferometer only measures phase differences between wave fronts arriving at the different antennas, the interferometer is only sensitive to differences in the TEC and is thus a spatial frequency filter for the ionosphere.

1.3 Contributions to Interferometric Phase

There are a number of general sources of phase corruption contributing to interferometric measurements that must be accounted for in order to determine the ionospheric components:

$$\phi(t) = \phi_{VLA} + \phi_{src}(t) + \phi_{ion}(t).$$

The first source of phase corruption is the instrument itself (ϕ_{VLA}). The electrical paths through the various electronics and transmission media are generally not well measured and so will introduce phase errors. The usual practice is to determine the instrumental component of the phase from astronomical observations. At low frequencies this process can be quite involved.

A second source of interferometric phase is the time variable contribution from the source ($\phi_{src}(t)$), unless its spatial extent is very small compared to the fringe spacings of the interferometer. Fortunately, if the source truly dominates the field of view, traditional self calibration techniques are adequate to determine a model for the source structure. This model can be Fourier transformed to estimate the contribution of the source structure to the interferometric phase.

The final source of phase corruption considered here is the time variable ionosphere ($\phi_{ion}(t)$). The signals arriving at each interferometer element will have passed through a different path through the ionosphere and will have a different delay induced by the variable index of refraction of the ionosphere.

1.4 Deriving Ionospheric Phases

At frequencies above a few tens of MHz, the ionosphere is essentially transparent and so only phase effects are considered below. As described in section 1.3, the phase of interferometer visibilities consist of a number of components. Several calibration steps are needed to separate these components.

1.4.1 RFI

At low frequencies radio frequency interference (RFI) abounds. For this reason and because of the wide fields of view needed, low radio frequency observations are generally done in "spectral line" mode, i.e. with many frequency channels. This allows channels and times affected by RFI to be "flagged" or ignored. Many of the sources of RFI are communications signals and are relatively narrow band, hence, can be recognized by the increased power levels with respect to adjacent spectral channels. Other types of interference may be broadband but impulsive in time (e.g. radar) and can be recognized by their temporal behavior.

Due to the volume of data, it is generally impractical to examine and flag data visually so automated schemes are important. Schemes such as AIPS task FLGIT or Obit task AutoFlag are useful in searching for impulsive temporal or spectral behavior and flagging the offending data prior to subsequent processing.

1.4.2 Source Model

One of the components of interferometer phase is the contribution due to the structure of the source. For a dominant source, the closure properties employed by traditional self–calibration techniques are sufficient to remove the other phase errors and allow a structural model of the source to be derived. This can be done using AIPS task SCMAP or Obit tasks SCMap or Imager. The flux density of the model may need to be adjusted to a known value. The CLEAN components of this model can then be Fourier transformed to derive the source structural phase for a given interferometric observation.

1.4.3 External calibration

As mentioned above, low frequency observations are generally made with significant spectral resolution and the phase effects of propagation of the signals through the various amplifiers and filters causes frequency dependent amplitude and phase effects in the data. Since these depend on the electronics of each antenna/data path, they will differ from antenna to antenna. If uncorrected, these "bandpass" errors will cause non–closing effects in the data corrupting subsequent calibration steps. The correction of this effect, called "bandpass calibration" can be performed by determining the amplitude and phase of each spectral channel with respect to an average of a number of channels. This will give channel/antenna/data path specific amplitude and phase corrections that need to be applied in subsequent steps. The bandpass calibrator needs to be a very strong source that dominates the field of view, Cygnus A is quite suitable for this purpose.

Strong sources at low frequencies tend to be resolved, so a source model is needed to estimate and remove the source's contribution to interferometer phase prior to estimating bandpass corrections. AIPS task BPASS (or CPASS when it works) can perform bandpass calibration.

At centimeter wavelengths the usual procedure is to perform phase referencing observations on a calibrator near to the target field. The observed phases on the calibrator are a combination of the instrumental and atmospheric contributions to the phase which are presumed to be common to the calibrator and the target. At low frequencies, the instrumental phase will be approximately common to all observing directions (limited by phase errors in the primary beam response, amoung others) but the ionospheric contribution can vary strongly with direction. Application of calibrator phases to a target field will correct the instrumental component of the phase but add the ionospheric component potentially making the phase corruption far worse. Thus, if spatially variant ionospheric phase is a significant problem, applying external phase calibration is a bad idea.

1.4.4 Self calibration of a bright source

After making bandpass and source structure phase corrections, the remaining interferometric phase is a combination of instrumental and ionospheric phases. For observations in which a single source dominates the field of view, the ionospheric contribution to each baseline phase is proportional to the difference in electrical path from the source to the two interferometer elements. This means that the interferometer phases are comprised of antenna/data path dependent terms which can be estimated by traditional (self) calibration procedures. Calibration programs such as AIPS CALIB or Obit Calib separate bandpass and source structure corrected data into time variable antenna/data path components.

1.4.5 Separation of contribution to the phase

At each time, the antenna/data path phases derived by the previous step consist of a number of components. Each antenna/data_path will have an instrumental phase which is, hopefully, constant in time. In addition, the ionospheric component of phase can be thought of as a phase screen across the array which is variable in time and space. For practical purposes, it is useful to split this phase screen into two components, a single phase gradient across the array and all the higher order terms. The gradient is essentially refraction and can be systematic in time (i.e. elevation) whereas the higher order terms have shorter time scales and, given enough sampling, should average to zero.

The technique to separate instrumental and ionospheric phase then becomes one of modeling the data as a constant set of instrumental phases and a time dependent 2D phase gradient for the whole array leaving the higher order terms as "residuals". If the data to be fitted contains sufficient temporal sampling, the higher order terms will average to zero leaving accurate estimates of the instrumental phases.

It should be noted that the results from this procedure are not unique. The phases corresponding to an arbitrary gradient can be added to the instrumental phases and subtracted from all gradient solutions and leave the same set of higher order residuals. Thus, the instrumental phases have had an arbitrary gradient added and the ionospheric phases an arbitrary gradient removed. The effect on imaging of using the derived instrumental phases is of a constant position offset.

Since the phases from the calibration procedure are ambiguous by multiples of turns, the fitting is nonlinear. The robustness of nonlinear fitting depends on the initial estimates of the parameters. The following describes the implementation in the Obit task SNFilt.

One of the parameters specified to SNFilt is a time range over which the ionosphere is relatively well behaved. This is usually determined from a visual inspection of the time sequences of phase derived from the phase calibration procedure above. It is desirable that this be a period over which the higher order phases are relatively small. The initial values for the instrumental phases are the average interferometer phases. These phases will also include the average gradient over the array during the specified time interval.

After applying the initial instrumental phases, the initial time series of phase gradients is estimated one at a time using a two step procedure. A phase gradient corresponds to a position

shift (Fourier shift theorem) and this is used in the initial guess for the gradient. The first step is to convert the antenna phases into pseudo visibilities with unit amplitude and phases which are the difference in antenna phases. This pseudo–data is then imaged using a direct cosine transform and the location of the peak in the derived image is converted into the corresponding phase gradient. This coarse estimate of the gradient is then refined using a least squares procedure independently for each time sample. In this least squares fitting, the residuals are constrained to be in the interval $[-\pi, \pi]$ by adding or subtracting multiples of 2π.

Following the initial parameter estimation, a global least squares procedure is performed for the constant instrumental phases and the time variable gradients. Residuals were constrained to $[-\pi, \pi]$ as above.

Following this, each time interval is examined and if the RMS phase residual exceeds a specified value, that interval is removed from the data set. If any time intervals are removed, the global fitting is repeated.

The final step is the generation of a new "solution" table with the phases replaced by either the instrumental phases or the residual phases with the optional inclusion of the phases from the gradients. For imaging purposes, the instrumental phases are used and for studying the effects of the ionosphere, the residuals are used.

1.5 Phase Movies

The residual phases derived from the previous procedure can be visualized by averaging and projecting onto the plane of the array. If there are multiple data paths (polarization products, "IFs" in VLA speak) or averaging in time is needed, then averages of the sine and cosine of the phases avoid the ambiguity problem. The average sines and cosines are then converted into phases and projected onto the plane of the array and can then be visualized. A time sequence of such images can then be visualized as a "movie" of the phase behavior over the array. This is implemented in Obit task IonMovie.

1.6 Phase Structure Function

One of the statistical properties of the ionospheric screen as projected onto the array is its structure function which here is taken to be

$$struc\_func(x) \ = \ < (\phi(x_0) - \phi(x_0 + x))^2 >$$

where x and x_0 are positions in the array. The square root of the structure function is easier to interpret as it is the RMS phase difference as a function of separation and this is what is implemented in Obit task IonSF. IonSF produces a "waterfall" image (with time flowing upwards) from an ionospheric phase movie with each row of the image corresponding to the square root of the structure function of one frame of the movie. Thus, the time behavior of the spatial coherence of the ionosphere can be visualized. This visualization can either include or not the estimated phase gradient. In the latter case, the troublesome higher order terms dominate but the results are sensitive to accurate fitting of the gradients which may fail when the higher order terms become large.

1.7 Examples

In the following, several examples are shown derived from extended observations of Cygnus A with the VLA at 74 MHz [3] in the A (35 km) configuration, with and without the addition of the VLBA Pietown antenna (70 km).
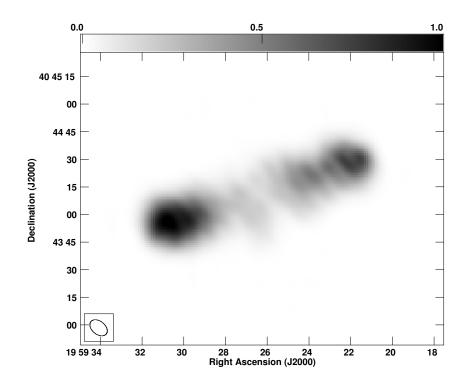
Figure 1.1: Image of Cygnus A derived from the VLA + VLBA Pietown at 74 MHz. (Courtesy of A. Cohen). The gray-scale is shown by the scale bar at the top. The resolution is shown in the lower left.

1.7.1   Model of Cygnus A

The model of Cygnus A used to calibrate the results described here is shown in Figure 1.1. This model uses the full resolution of the VLA plus VLBA Pietown.

1.7.2   Phase Movie

The time sequence of phase images is best visualized as a movie but some of the major features can be seen in a sequence of images represented in Figure 1.2. This sequence was derived from observations of Cygnus A during a moderately active period; the estimate of the ionospheric gradient has been removed leaving only higher order terms. The reference antenna was the first antenna on the north arm so the phases are near zero at the center of the array. In this sequence, the phase has a strong negative gradient along each of the arms at the beginning of this two minute sequence and by the end, the phase has a positive gradient along each arm. In the middle of this sequence, the phases are well represented by a 2D gradient but there is significant curvature at the beginning and end. This is shown in the structure functions shown in Figure 1.3 where the values of the residual structure function are small. At the beginning and end of the sequence the structure function has RMS phase deviations from a 2D gradient of order 80° on some size scales.

1.7.3   Structure Function

The use of structure function images was introduced in the previous section to show their relation to the distribution of phase over the array. These figures can also be used to illustrate the behavior of the ionosphere over longer periods of time.
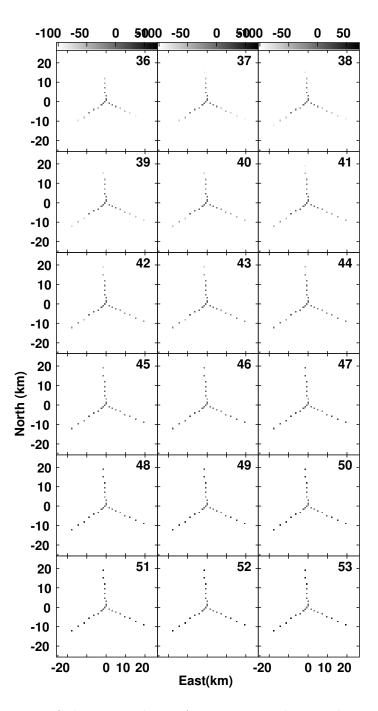
Figure 1.2: Time sequence of phase over the VLA in 6.67 second intervals. Note the phase at the ends of all arms change from $\sim -100°$ to $\sim +70°$. The gray-scale is shown by the scale bar at the top.
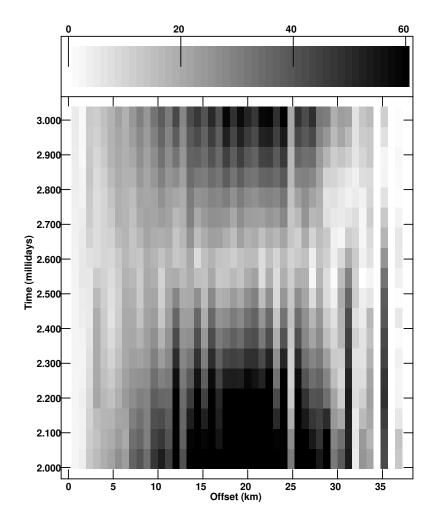
Figure 1.3: Waterfall plot of the structure functions derived from the data shown in Figure 1.2. Units are degrees with the scale shown by the scale bar at the top.

Moderate activity

Figure 1.4 shows the structure functions for a period of relatively quiet ionospheric activity. The left plot shows the structure function without removal of the fitted ionospheric gradients and on the right is the same data with the fitted gradients removed. During periods of enhanced activity, the gradient fitting can fail.

The fringing in Figure 1.4 is due to the phase being constrained to the range [-180,180] so the "structure function" goes to zero for exactly n turns of phase difference. This feature can be useful as a pure position shift give this strong fringing appearence whereas when it's more complicated the fringing goes away.

Serious activity

On a day of higher ionospheric activity the structure functions are more chaotic as is shown in Figure 1.5. A comparison of the left and right figures shows that while much of the ionospheric structure can be modeled with a simple gradient, a large amount remains on essentially all size scales sampled. Note the weak "fringing" appearance as compared to Figure 1.4. In cases of strong ionospheric activity such shown here, the fitting of the instrumental phases may be questionable.

Extending the baselines to 70 km

The offset range of the structure functions sampled can be extended, if sparsely, using measurements including the VLBA antenna at Pietown NM. Data taken on a moderately active day is shown in Figure 1.6. Due to the longer baselines, the gradient fitting sometimes produces poor results but for much of the time and offset space, the RMS phase residuals from a gradient are under a radian.

1.8   Conclusions

This study has shown that potentially useful measurements of the statistical properties of the ionospheric phase screen can be derived from low frequency observations of a very bright source. The lines of sight from each of the antennas to the source map a pattern of puncture lines on the ionospheric screen. An accurate model of the source being observed is needed to remove the source structural contributions to the measured visibility phase. A standard calibration can then reduce the observed visibility phases into their antenna based components. The principal difficulty is separating the instrumental contributions to the phase from the ionospheric contributions. The instrumental phases cannot be determined uniquely from astronomical observations and will include a component due to ionospheric refraction.

A model fitting of the antenna phases can be used to determine one of the families of instrumental phases as well as an estimate of the overall refractive phase gradient. This procedure requires that sufficient observations be obtained that the higher order terms average to zero.

Given the antenna–based phases with instrumental phases removed and either with or without the estimate of the overall gradient removed, the phases can be projected onto the plane of the array to get the image of the ionospheric phase screen on the ground. A time sequence of such images produces an "ionospheric movie" which can be used to help understand the properties, sizes and timescales of ionospheric structures.

Structure functions give a statistical measure of the structure of the ionospheric phase screen on various size scales. This collapse of the 3D "movies" to a 2D image provides a tool to visualize the temporal and spatial nature of the phase screen. Structure functions derived from data from which the estimated refractive gradient has been removed give a better idea of the smaller scale ionospheric structures but only work well when the ionosphere is not so disturbed that a refractive
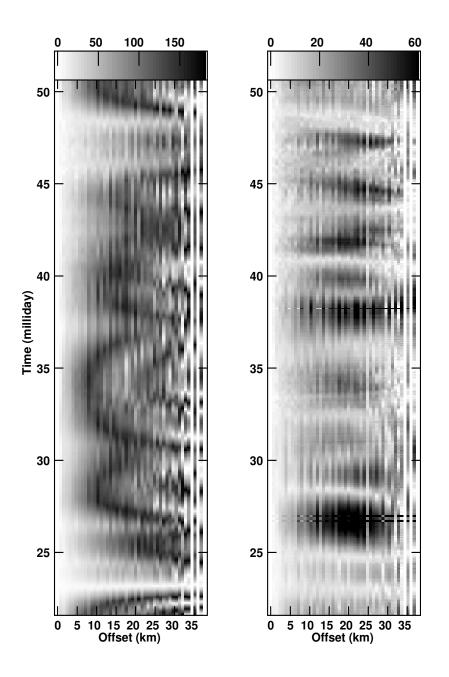
Figure 1.4: **Left**: Waterfall plot of the structure functions derived from an extended observation of Cygnus Aduring a period of modest ionospheric activity.. No ionospheric gradient was removed. Units are degrees with the scale shown by the scale bar at the top.
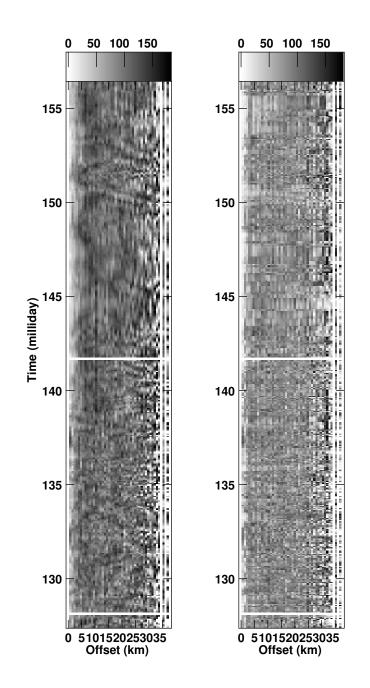**Right**: Same data as **Left** but with ionospheric gradients removed.

Figure 1.5: **Left**: Waterfall plot of the structure functions derived from an extended observation of Cygnus A during relatively high levels of ionospheric activity. No ionospheric gradient was removed. Units are degrees with the scale shown by the scale bar at the top.
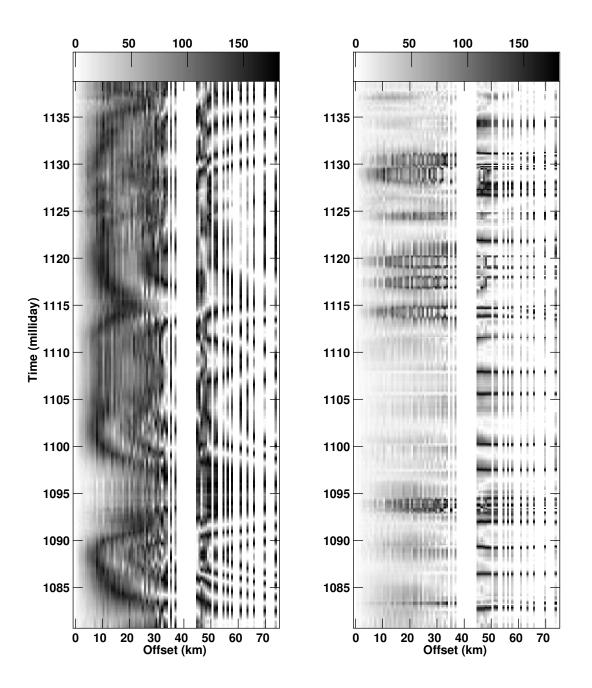**Right**: Same data as **Left** but with ionospheric gradients removed.

Figure 1.6: **Left**: Waterfall plot of the structure functions derived from an extended observation of Cygnus A using the VLA plus the VLBA Pietown antenna. No ionospheric gradient was removed. Units are degrees with the scale shown by the scale bar at the top.
Right: Same data as **Left** but with ionospheric gradients removed.

wedge gives a poor fit to the data. Using higher order models of the phase screen may be a useful refinement of these techniques.

1.9 Acknowledgments

Bibliography

[1] W. D. Cotton. Lessons from the VLA Long Wavelength Sky Survey (VLSS). In *Science with Human Wavelengths, Astronomical Society of the Pacific Conference Series, vol, 345*, pages 337–340, 2005.

[2] W. D. Cotton, J. J. Condon, R. A. Perley, N. Kassim, J. Lazio, A. Cohen, W. Lane, and W. C. Erickson. Beyond the isoplanatic patch in the VLA Low-frequency Sky Survey. In *Proceedings of the SPIE, Volume 5489.*, pages 180–189, 2004.

[3] N. E. Kassim, T. J. Lazio, W. C. Erickson, R. A. Perley, W. D. Cotton, E. W. Greisen, A. S. Cohen, B. Hicks, H. R. Schmitt, and D. Katz. The 74 MHz System on the Very Large Array. *ApJ Suppl.*, Accepted, 2007.